

On Practical Robust Reinforcement Learning: Practical Uncertainty Set and Double-Agent Algorithm

Ukjo Hwang, *Student, IEEE*, and Songnam Hong, *Member, IEEE*

Abstract—We study a robust reinforcement learning (RL) with model uncertainty. Given nominal Markov decision process (N-MDP) that generate samples for training, an uncertainty set is defined, which contains some perturbed MDPs from N-MDP for the purpose of reflecting potential mismatched between training (i.e., N-MDP) and testing environments. The objective of robust RL is to learn a robust policy that optimizes the worst-case performance over an uncertainty set. In this paper, we propose a new uncertainty set containing more realistic MDPs than the existing ones. For this uncertainty set, we present a robust RL algorithm (named ARQ-Learning) for tabular case and characterize its finite-time error bound. Also, it is proved that ARQ-Learning converges as fast as Q-Learning and the state-of-the-art robust Q-Learning while ensuring better robustness to real-world applications. Next, we propose *pessimistic* agent that efficiently tackles the key bottleneck for the extension of ARQ-Learning into the case with larger or continuous state spaces. Incorporating the idea of pessimistic agents into the famous RL algorithms such as Q-Learning, deep-Q network (DQN), and deep deterministic policy gradient (DDPG), we present PRQ-Learning, PR-DQN, and PR-DDPG, respectively. Noticeably, the proposed idea can be immediately applied to other model-free RL algorithms (e.g., soft actor critic). Via experiments, we demonstrate the superiority of our algorithms on various RL applications with model uncertainty.

Index Terms—Reinforcement learning, robust reinforcement learning, robustness, uncertainty set.

I. INTRODUCTION

In Markov decision process (MDP) and reinforcement learning (RL) [1], [2], it is commonly assumed that a testing (or true) environment on which a learned policy will be deployed is the identical to a training environment that was used to construct the policy. In practice, however, it is often violated due to the simulator modeling errors (i.e., the mismatch between the training and the true environment), environment changes in real system dynamics over time, and unpredictable events. Such deviation can result in significant performance degradation. To address this problem, the framework of robust MDP (R-MDP) was introduced in [3]–[5], where the transition kernel of the MDP is not fixed and lies in the so-called *uncertainty set*. The goal of R-MDP is to seek a policy that performs well under the worst-case MDP in the uncertainty set. In [3]–[5], model-based approach was assumed and accordingly, uncertainty set is known beforehand. Likewise classical MDP,

dynamic programming can be used to find the optimal robust policy.

The model-based approach requires a model of the transition kernel and the uncertainty set beforehand, which makes it less applicable for many real-world applications. Motivated by this, (model-free) robust RL with model uncertainty was recently proposed in [6]–[9], which aim at learning a robust policy using a simple trajectory from nominal MDP (N-MDP) (or training environment), e.g., a simulator and a similar environment in which samples are easier to collect than in the testing (or true) environment where the policy is going to be deployed. To take into account the impact of such mismatches, an uncertainty set is defined by containing all possible *perturbed* MDPs from N-MDP [6]–[9]. Since N-MDP is not given beforehand, the uncertainty set and an optimal robust policy should be learned simultaneously using sequentially observed data samples from N-MDP. Thus, if the uncertainty set is well-constructed, a learned robust policy can guarantee the robustness to some unexpected events in real-world environments. The major challenges of robust RL are twofold: i) an uncertainty set must be well-designed to take into account real-world uncertainties (or perturbations) precisely; ii) given the uncertainty set, a robust policy should be efficiently learned via data samples from N-MDP in an online fashion. We contribute to this subject.

A. Related Work

In this section, we briefly review the existing robust RL approaches.

Model-Based R-MDP. The framework of R-MDP was studied in [5], [10], [11], which can be solved via dynamic programming using the knowledge of the transition kernel and the predefined uncertainty set. This approach based on tabular case was further extended to the case with function approximation [12]. These methods cannot be applied to our work as in this paper, (model-free) RL is considered, i.e., the transition kernel of N-MDP and the uncertainty set are not defined and instead, they should be simultaneously learned only using data samples from N-MDP.

Adversarial Robust RL. In [5], it was shown that robust MDP problem is equivalent to a zero-sum game between the agent and the nature. Based on this, adversarial training approach was investigated in [13]–[17], where the state transition can be *perturbed* by an adversary agent. Namely, in this adversary approach, the state transition can be modified in an arbitrary

U. Hwang and S. Hong are with the Department of Electronic Engineering, Hanyang University, Seoul, 04763, Korea (e-mail: {yd1001, snhong}@hanyang.ac.kr)

way. In [18]–[21], the current state was modified from adversarial samples. Thus, during the training, adversarial robust RL approaches need to manipulate the state transition of N-MDP. Whereas, robust RL with model uncertainty, which is the subject of this paper, does not require such manipulation during the training.

Model-Free Robust RL. In [8], [9], model-free robust RL with model uncertainty was investigated, where the uncertainty is constructed using confidence region consisting of some constraints on probability distributions. Leveraging this uncertainty set, the authors developed robust RL algorithm by means of linear function approximation. However, in model-free RL (i.e., N-MDP is unknown), it is challenging to describe a confidence region. Consequently, under this uncertainty set, it was failed to find an optimal robust policy efficiently. Instead, a proxy confidence region was introduced, which is obtained by relaxing some conditions. Using the proxy, an efficient robust algorithm was developed but there is no theoretical guarantee for the exactness of such approximation. Very recently in [6], [7], robust RL algorithm was developed by constructing the uncertainty set via Huber’s R -contamination set [22]. This is the most related work of our paper. Unlike [8], [9], this uncertainty set does not require any condition for probability distributions, which makes it possible to develop model-free robust RL algorithm without any relaxation. Beyond the asymptotic analysis, the finite-time error bound for this algorithm was derived [6]. Nonetheless, this uncertainty set still poses the limitation as it includes several unrealistic perturbed MDPs (i.e., unpractical state transitions). In real-world applications, these unrealistic ones are indeed infeasible (see Section III-A for details). Furthermore, their experiments were very restricted and did not extend to continuous action space environments. In this paper, we address this limitation by presenting a new practical uncertainty and an efficient robust RL algorithm for continuous state/action spaces.

B. Our Contributions

We first present an *adjacent* R -contamination uncertainty set by elaborating the famous R -contamination uncertainty set [6], [7] in a more practical way. As noticed in I-A, despite its tractability, the limitation of the existing uncertainty set is to contain some unrealistic state transitions as potential perturbations. Specifically, it allows any current state to transit to every state in the state space with non-zero probability. Whereas, the proposed uncertainty set only allows that a state can transit to the states belonging to its neighboring set which includes the states with non-zero transition probabilities from N-MDP. Our uncertainty set is more reasonable in the premise that training environment (i.e., N-MDP) is constructed to reflect testing environment as much as possible. As an example, a drone flying in the air can be pushed by some unexpected air-flow from any direction and with any strength. The proposed uncertainty set assumes that the drone can move nearby due to the unexpected movement while the existing one assumes that it can move anywhere (i.e., far away). For the proposed adjacent R -contamination uncertainty set, we derive the robust Bellman operator, which plays a key

role in developing robust RL algorithms. Leveraging this, we propose a sample-based algorithm (named ARQ-Learning) for tabular case. We theoretically prove that it can converge as fast as vanilla Q-Learning [23] and the-state-of-the-art robust Q-Learning [6] while ensuring better robustness to real-world applications.

However, it is demanding to extend ARQ-Learning into the cases with larger or continuous state spaces for the following reason. Compared with the conventional Bellman operator, our robust Bellman operator includes an additional maximization term. Also, the complexity to solve the maximization grows exponentially with the size of state space. The same problem has been happened in robust Q-Learning [6]. For the proposed uncertainty set, we address this problem by introducing pessimistic agent (a.k.a. max-solver). The objective of pessimistic agent is to efficiently solve the aforementioned maximization using data samples from training environment in an online and incremental fashion. Incorporating the idea of pessimistic agent into ARQ-Learning, we propose a new robust Q-Learning, named PRQ-Learning, for tabular case with large state spaces. We emphasize that the idea of pessimistic agent enables to harness function approximation (e.g., deep-neural-network (DNN)) for the design of robust RL algorithms. Based on this, we propose PR-DQN for continuous state spaces and PR-DDPG for continuous state and action spaces, by combining our idea with the popular deep-Q network (DQN) [24] and deep deterministic policy gradient (DDPG) [25], respectively. This extension makes it possible to employ robust RL framework in various real-world applications. It is remarkable that the proposed idea to use pessimistic agent can be immediately applied to the other model-free RL algorithms such as soft-actor-critic (SAC) [26], twin delayed deep deterministic policy gradient (TD3) [27] and proximal policy optimization (PPO) [28].

Via experiments, we demonstrate the superiority of our algorithms on various RL applications with some perturbations (or mismatches). For the first time, we implemented robust RL algorithms with DNN-based function approximations, while in the existing work [6], a simple linear function approximation was only considered. As aforementioned, the idea of pessimistic agent makes it possible to use complex DNNs as function approximation. We remark that our idea to use pessimistic agent is customized to the proposed uncertainty set, namely, it cannot be applied to the existing algorithms in [6] due to the difference of uncertainty sets. From experimental results, we observe that the proposed algorithms can achieve much higher rewards than (vanilla) RL and the-state-of-the-art robust RL algorithms, when testing environment has some perturbations compared with training environment. This implies that the proposed algorithms indeed ensure the robustness against the unknown perturbations in testing environment. Also, these results strengthen our argument that our adjacent R -contamination uncertainty set better reflects real-world perturbations than the existing set [6]. Furthermore, since it is confirmed that the idea of pessimistic agent performs well, i.e., it can solve the maximization precisely, the combination of our idea with various RL algorithms would produce a good candidate for robust RL framework.

C. Paper Organization

The remaining part of this paper is organized as follows. In Section II, we formally define a robust RL with an uncertainty set. In Section III, we present a new practical uncertainty set (named adjacent R -contamination uncertainty set) and derive the corresponding robust Bellman operator, which is the key for the design of robust RL algorithms. In Section IV, leveraging the robust Bellman operator, we design an efficient robust RL algorithm (named ARQ-Learning) for tabular case and theoretically characterize its finite-time error bound. Also, pessimistic agent is introduced, which can tackle the key bottleneck for the extension of ARQ-Learning into larger and continuous state space. As a consequence, PRQ-Learning is proposed for tabular case with larger state spaces. Combining our idea with the popular RL algorithms as DQN and DDPG, PR-DQN and PR-DDPG are respectively presented in Section V for continuous state spaces. In Section VI, we demonstrate the superiority of our algorithms via experiments on real-world RL applications with some perturbations. Some concluding remarks are provided in Section VII.

II. PRELIMINARIES

We provide some definitions that will be used throughout the paper and formally define a robust reinforcement learning (RL) with model uncertainty.

MDP. A Markov decision process (MDP) is defined with a tuple $(\mathcal{S}, \mathcal{A}, \mathbf{P} = (p_{s,s'}^a), c, \gamma)$, where \mathcal{S} is the state space, \mathcal{A} is the action space, \mathbf{P} is the state transition kernel, $c: \mathcal{S} \times \mathcal{A} \rightarrow \mathbb{R}$ is the cost function, and $\gamma \in (0, 1)$ is the discount factor. Here, $p_{s,s'}^a$ represents the probability of transition to state $s' \in \mathcal{S}$ when action $a \in \mathcal{A}$ is taken at the current state $s \in \mathcal{S}$. For ease of notation, we let $p_s^a = (p_{s,s'}^a)$ denote the probability distribution on the possible next state $s' \in \mathcal{S}$, given the current state s and action a . At every time step t , an agent observes the environment's state s_t and takes an action a_t according to the agent's policy $\pi: \mathcal{S} \times \mathcal{A} \rightarrow [0, 1]$. Then, the environment moves to a next state s_{t+1} according to $p_{s_t, s_{t+1}}^{a_t}$ and generates a cost $c(s_t, a_t)$. Given a state $s \in \mathcal{S}$, the value function of a policy π is evaluated as

$$V_{\mathbf{P}}^{\pi}(s) = \mathbb{E}_{\pi, \mathbf{P}} \left[\sum_{t=0}^{\infty} \gamma^t c(s_t, a_t) \middle| s_0 = s \right], \quad (1)$$

where $a_t \sim \pi(s_t)$ and $s_{t+1} \sim p_{s_t}^{a_t}$. Given the MDP $(\mathcal{S}, \mathcal{A}, \mathbf{P} = (p_{s,s'}^a), c, \gamma)$, the objective of RL is to find an optimal policy π^* such that

$$\pi^* = \operatorname{argmin}_{\pi} V_{\mathbf{P}}^{\pi}(s), \quad \forall s \in \mathcal{S}. \quad (2)$$

Robust MDP. In robust MDP, there is some uncertainty in an environment for which the state transition kernel \mathbf{P} is not fixed but can be changed (or perturbed) at every time step [6], [8], [9]. This uncertainty can be captured by an uncertainty set \mathcal{P} that contains all possible *perturbed* state transition kernels. As in [5], [6], [10], it is commonly assumed that the uncertainty set has the form of

$$\mathcal{P} = \bigotimes_{(s,a) \in \mathcal{S} \times \mathcal{A}} \mathcal{P}_s^a, \quad (3)$$

where \mathcal{P}_s^a includes all perturbed transition distributions of a next state s' given the current state s and action a . Given the set \mathcal{P} , a robust MDP (**R-MDP**) is specified as $(\mathcal{S}, \mathcal{A}, \mathcal{P}, c, \gamma)$. As aforementioned, in robust RL, the training environment (a.k.a., nominal MDP (**N-MDP**) $(\mathcal{S}, \mathcal{A}, \bar{\mathbf{P}} = (\bar{p}_{s,s'}^a), c, \gamma)$) is defined, from which samples for training are assumed to be generated. Let \mathbf{P}_t be the state transition kernel at time step t and $\kappa = (\mathbf{P}_0, \mathbf{P}_1, \dots)$ be a sequence of state transition kernels.

In robust RL, one key challenge is to build an uncertainty set such that i) it can reflect real-world mismatches; ii) it is manageable to find an optimal robust policy via an efficient algorithm. We contribute to this subject in Section III - Section V. Given an uncertainty set \mathcal{P} , robust RL seeks an optimal robust policy π^* to minimize the cumulative discounted cost over all state transition kernels in the uncertainty set. In the remaining part of this section, we provide some definitions and notations that will be used to tackle the above problem. Given the state s , the *robust* state value function of a policy π is defined as

$$V^{\pi}(s) = \max_{\kappa} \mathbb{E}_{\pi, \kappa} \left[\sum_{t=0}^{\infty} \gamma^t c(s_t, a_t) \middle| s_0 = s \right], \quad (4)$$

where \mathbb{E}_{κ} denotes the expectation when state transitions follow κ . Also, given the state s and action a , the *robust* action value function of a policy π is defined as

$$Q^{\pi}(s, a) = \max_{\kappa} \mathbb{E}_{\pi, \kappa} \left[\sum_{t=0}^{\infty} \gamma^t c(s_t, a_t) \middle| s_0 = s, a_0 = a \right]. \quad (5)$$

The optimal policy of robust MDP is defined as

$$\pi^* = \operatorname{argmin}_{\pi} V^{\pi}(s), \quad \forall s \in \mathcal{S}. \quad (6)$$

For ease of expositions, we let V^* and Q^* denote the optimal value functions, which implies V^{π^*} and Q^{π^*} , respectively. The optimal value functions have the relation such as

$$V^* = \min_{a \in \mathcal{A}} Q^*(s, a). \quad (7)$$

Remark 1: One can concern the aforementioned dynamic model, which allows the transition kernel to be time-varying, since the majority of real-world settings differ from the training environment in an unpredictable way but fixed throughout the episode. In [5], it was shown that the dynamic model is equivalent to the static model, where the transition kernel is static, namely, $\mathbf{P}_{t_1} = \mathbf{P}_{t_2}$ for any t_1, t_2 (i.e., fixed throughout the episode), under a general condition that the agent's policy is stationary and the problem is infinite horizon with discounted reward. Therefore, an optimal robust policy under the time-varying model is also optimal for the static model.

III. PROPOSED ROBUST RL FRAMEWORK

In this section, we introduce a new uncertainty set which is more practical and precise than the existing sets. Then, we derive the robust Bellman operator \mathbf{T} for the proposed uncertainty set \mathcal{P} .

A. Proposed Uncertainty Set

We describe the proposed uncertainty set for robust RL. Since N-MDP is unknown, it is unable to generate samples (or trajectories) directly from perturbed transition kernels $\mathbf{P}_t \in \mathcal{P}$. On constructing an uncertainty set, thus, it should be considered to develop an efficient way to mimic such samples only using data samples from N-MDP. Thus, it is demanding to train a robust agent from R-MDP with a general uncertainty set. For this reasons, the two types of tractable uncertainty sets have been widely used:

- A confidence region-based uncertainty set [8], [9]: For $\forall(s, a) \in \mathcal{S} \times \mathcal{A}$,

$$\mathcal{P}_s^a \triangleq \{\bar{p}_s^a + u \mid u \in \mathcal{U}_s^a\}, \quad (8)$$

where

$$\mathcal{U}_s^a = \left\{ x \mid \|x\|_2 \leq R, \sum_{s' \in \mathcal{S}} x_{s'} = 0, \right. \\ \left. -\bar{p}_{s,s'}^a \leq x_{s'} \leq 1 - \bar{p}_{s,s'}^a, \forall s' \in \mathcal{S} \right\}.$$

- R -contamination uncertainty set [6], [7]: For $\forall(s, a) \in \mathcal{S} \times \mathcal{A}$,

$$\mathcal{P}_s^a \triangleq \{(1 - R)\bar{p}_s^a + Rq \mid q \in \Delta_{|\mathcal{S}|}\}, \quad (9)$$

where $\Delta_{|\mathcal{S}|}$ is the $(|\mathcal{S}| - 1)$ -dimensional probability simplex.

In both cases, the state transition probability \bar{p}_s^a from N-MDP is adopted as the centroid and a hyperparameter $R \in [0, 1]$ denotes a robustness level. Based on these uncertainty sets, robust RL algorithms have been well-investigated [6]–[9].

We remark that these uncertainty sets have the limitation to describe real-world situations. Generally, in real environments, a state s cannot transit to every state $s' \in \mathcal{S}$, namely, it can only transit to some states (called neighboring states). In the example of CliffWalking (see Fig. 1), an agent can only move in 4 directions and accordingly, it can only reach to the 4 neighboring states. When the uncertainty set in (8) or (9) is used, however, the most of perturbed MDPs in the uncertainty set allows that any state s can transit to the overall states with non-zero probabilities. To rule out these unrealistic state transitions, an uncertainty set must be more carefully designed.

This motivates us to present a new uncertainty set, named *adjacent R -contamination uncertainty set*:

Definition 1: Given N-MDP $(\mathcal{S}, \mathcal{A}, \bar{\mathbf{P}} = (\bar{p}_{s,s'}^a), c, \gamma)$ which generates samples for training, we define an *adjacent R -contamination uncertainty set*: for $\forall(s, a) \in \mathcal{S} \times \mathcal{A}$,

$$\mathcal{P}_s^a \triangleq \{(1 - R)\bar{p}_s^a + Rq \mid q \in \mathcal{Q}_s\}, \quad (10)$$

where \mathcal{Q}_s contains all feasible conditional distributions:

$$\mathcal{Q}_s \triangleq \{q \in \Delta_{|\mathcal{S}|} \mid q_{s'} = 0, \forall s' \in \mathcal{S} - \mathcal{N}_s\} \subseteq \Delta_{|\mathcal{S}|}, \quad (11)$$

and the neighboring set of a state $s \in \mathcal{S}$ is defined as

$$\mathcal{N}_s \triangleq \left\{ s' \in \mathcal{S} \mid \sum_{a \in \mathcal{A}} \bar{p}_{s,s'}^a \neq 0 \right\}. \quad (12)$$

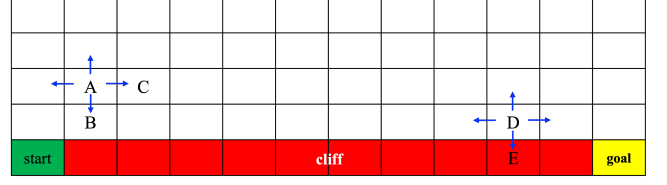


Fig. 1. A grid-world with cliff (or CliffWalking-v0), where agent aims to reach the goal. Here, green represents start state, yellow represents goal, and red represents cliff which gives highest cost.

Note that when $R = 0$, \mathcal{P} is the singleton with $\{\bar{\mathbf{P}}\}$, namely, in this case, robust RL is reduced to vanilla RL.

Definitely, the proposed uncertainty set is the subset of the R -contamination uncertainty set in (9). We argue that the former takes only realistic state transitions from the latter, given the premise that infeasible transitions in N-MDP are more likely to be still infeasible in the testing environment. We provide an example to convince our argument. In Fig. 1, suppose that an agent at the state ‘A’ intends to move to the state ‘C’ according to the policy. Due to some unpredictable event in the testing environment, the agent can move to unwanted state ‘B’ (i.e., one of the neighboring states). However, it is unreasonable to assume that the agent at the state ‘A’ can move to the state ‘D’ or ‘E’ directly in one step. This unrealistic movement is prevented in our uncertainty set, whereas it is allowed with non-zero probability in the existing uncertainty sets in (8) and (9). Thus, the proposed uncertainty set in (10) can reflect real-world environments more elaborately than the existing ones. Despite its superiority, it is nontrivial to construct an efficient robust RL algorithm based on the proposed uncertainty set. This will be completely addressed in Section IV and Section V for tabular and function-approximation cases, respectively.

B. Robust Bellman Operator

On constructing RL algorithms, Bellman operator is commonly used for policy evaluation steps. Likewise, we need to define the robust Bellman operator for robust MDP with the proposed uncertainty set in (10). In [4], given an uncertainty set \mathcal{P}_s^a , the robust Bellman operator is derived as

$$\mathbf{T}Q^\pi(s, a) = c(s, a) + \gamma \sigma_{\mathcal{P}_s^a}(V^\pi), \quad (13)$$

where $\sigma_{\mathcal{P}_s^a}(v) \triangleq \max_{p \in \mathcal{P}_s^a} p^\top v$ is the support function of \mathcal{P}_s^a . We note that this Bellman operator holds for the uncertainty sets in (8), (9), and (10). In particular, the robust Bellman operator for the proposed uncertainty set in (10) is derived as

$$\mathbf{T}Q^\pi(s, a) = c(s, a) + \gamma(1 - R) \left[\sum_{s' \in \mathcal{S}} \bar{p}_{s,s'}^a V^\pi(s') \right] \\ + \gamma R \left[\max_{s' \in \mathcal{N}_s} V^\pi(s') \right], \quad (14)$$

where $R \in [0, 1]$ is a robustness-level, \mathcal{Q}_s and \mathcal{N}_s are given in Definition 1.

We theoretically prove the asymptotic convergence of our robust Bellman operator in (14), namely, the proposed un-

certainty set also guarantees a theoretical convergence as the conventional R -contamination uncertainty set in [6].

Theorem 1: For any $\gamma \in (0, 1)$ and $R \in [0, 1]$, the Bellman operator \mathbf{T} in (14) is a contraction with respect to l_∞ -norm, and the robust value function Q^π has its unique fixed point.

Proof: The proof is provided in Appendix A. ■

Leveraging (14), we will design sample-based robust RL algorithms for tabular and function-approximation cases in Section IV and Section V, respectively.

IV. PROPOSED TABULAR METHODS

Focusing on the tabular case with finite state and action spaces, we will devise the robust RL algorithms with the proposed adjacent R -contamination uncertainty set in (10).

A. ARQ-Learning

Using the robust Bellman operator in (14), one can expect to develop Q-Learning algorithm. Unlike vanilla RL, however, the maximization over neighboring states in (14) should be additionally tackled. Regarding this maximization, we should address the two requirements during the training:

- (i) Given a state $s \in \mathcal{S}$, the neighboring set \mathcal{N}_s should be identified only using the data samples from the training environment.
- (ii) Using the neighboring set \mathcal{N}_s , the maximization in (14) should be efficiently solved.

First, we focus on the requirement (i). To identify the neighboring sets \mathcal{N}_s for $\forall s \in \mathcal{S}$ using data samples from the training environment, we define an indicator transition matrix (ITM), denoted by $\mathbf{B} \in \{0, 1\}^{|\mathcal{S}| \times |\mathcal{S}|}$, where the (i, j) -component of \mathbf{B} (i.e. $\mathbf{B}_{i,j}$) is equal to 1 if the state transition from the state i to the state j can occur with non-zero probability in N-MDP. During the training, \mathbf{B} is estimated using data samples in an online fashion. For example, starting with all-zero matrix, $\mathbf{B}_{i,j}$ is set by 1 as long as the sample that transit the state i to the state j occurs. Then, from the up-to-date \mathbf{B} , we can build an estimated neighboring set as

$$\hat{\mathcal{N}}_s = \{s' \in \mathcal{S} \mid \mathbf{B}_{s,s'} \neq 0\}. \quad (15)$$

Clearly, we have $\hat{\mathcal{N}}_s \subseteq \mathcal{N}_s$ and after sufficient time steps, it is expected that $\hat{\mathcal{N}}_s \approx \mathcal{N}_s$ for $\forall s \in \mathcal{S}$. Using the estimated neighboring sets and the robust Bellman operator in (14), the update of our robust Q-Learning with sample $(s_t, a_t, c_t = c(s_t, a_t), s_{t+1})$ is derived as follows:

$$Q_{t+1}^\pi(s_t, a_t) \leftarrow (1 - \alpha)Q_t^\pi(s_t, a_t) + \alpha \left(c_t + \gamma R \max_{s' \in \hat{\mathcal{N}}_{s_t}} V_t^\pi(s') + \gamma(1 - R)V_t^\pi(s_{t+1}) \right), \quad (16)$$

where $\alpha > 0$ is a learning rate. Based on this update, we propose **Adjacent Robust Q-Learning (ARQ-Learning)**, which is described in Algorithm 1. Remarkably, it can perform only using data samples from the training environment. To compare

Algorithm 1 ARQ-Learning

```

1: Input: Learning rate  $\alpha > 0$ , discounted factor  $\gamma \in (0, 1)$ ,
   and robustness-level  $R$ .
2: Initialization:  $Q^\pi(\cdot, \cdot)$ ,  $\mathbf{B} = \mathbf{0}$ ,  $s_0 \in \mathcal{S}$ .
3: for each epoch do
4:   for each environment step do
5:      $a_t \sim \pi(s_t)$  and  $s_{t+1} \sim \bar{p}_{s_t}^{a_t}$ 
6:      $\mathcal{D} \leftarrow \mathcal{D} \cup \{(s_t, a_t, c_t, s_{t+1})\}$ 
7:      $\mathbf{B}_{s_t, s_{t+1}} \leftarrow 1$  and  $s_t \leftarrow s_{t+1}$ 
8:   end for
9:   for each update step do
10:     $(s, a, c, s') \sim \mathcal{D}$ 
11:     $V_t^\pi(s') = \min_{a' \in \mathcal{A}} Q_t^\pi(s', a')$ 
12:    Update  $Q^\pi$  via (16)
13:   end for
14: end for

```

with the most related work [6], the update of robust Q-Learning with R -contamination uncertainty set is derived as follows:

$$Q_{t+1}^\pi(s_t, a_t) \leftarrow (1 - \alpha)Q_t^\pi(s_t, a_t) + \alpha \left(c_t + \gamma R \max_{s' \in \mathcal{S}} V_t^\pi(s') + \gamma(1 - R)V_t^\pi(s_{t+1}) \right). \quad (17)$$

In comparison with the update of ARQ-Learning in (16), we observe that there is no state-dependent constraint for the maximization in (17). Specifically, in both cases, some additional terms are added so that Q-function is updated in a more conservative way. However, the adding terms are totally different such as $R \max_{s' \in \hat{\mathcal{N}}_{s_t}} V_t^\pi(s')$ for ARQ-Learning and $R \max_{s' \in \mathcal{S}} V_t^\pi(s')$ for robust Q-Learning, where the former is state-dependent while the latter is just constant regardless of a state s . This difference makes robust Q-Learning based on R -contamination uncertainty set [6] unable to consider an uncertainty in the testing environment properly.

To better understand our argument, we provide an example with Fig. 1. In this example, the state ‘E’ is likely to have higher value $V_t^\pi(s = \text{‘E’})$ as it is in the cliff. When evaluating the action value function of the state ‘D’, it makes sense to consider the danger of the neighboring state ‘E’ (i.e., $V_t^\pi(\text{‘E’})$) as the state ‘D’ has some possibility to move to the neighboring state ‘E’ by some unexpected events in the testing environment. On the other hand, when evaluating the action value function of the state ‘A’, it is unreasonable to take $V_t^\pi(\text{‘E’})$ into account as the state ‘A’ is far from the state ‘E’ (i.e., this transition is impossible in one step). Nonetheless, in robust Q-Learning [6], such unrealistic transition is reflected (i.e., $V_t^\pi(\text{‘E’})$ is considered) when evaluating (17) at the state ‘A’. Noticeably, this problem has been perfectly addressed in the updated of the proposed ARQ-Learning in 16 as ‘D’ is not the neighbor of ‘A’. Remarkably, ARQ-Learning only takes the realistic danger (caused by neighboring states) into account, when evaluating the action value function (see (16)). In addition, suppose that $V_t^\pi(\text{‘E’})$ is extremely high, which is highly likely to occur. The maximum state $\text{‘E’} = \operatorname{argmax}_{s \in \mathcal{S}} V_t^\pi(s)$ in (17) could be the same for the entire time steps. At every time step, the almost same value is added, which is nothing

but adding a constant at every time steps. Because of these reasons, the proposed uncertainty set is more adequate than the existing R -contamination uncertainty set.

Remark 2: One can concern that for a certain training environment, it would be possible that any state s can transit to all states $\forall s' \in \mathcal{S}$ and thus, the existing uncertainty sets (8) and (9) are proper ones for this environment. However, if such state transitions are possible, the corresponding neighboring set in (12) becomes the entire state space (i.e., $\mathcal{N}_s = \mathcal{S}$). Namely, our adjacent R -contamination uncertainty set (10) is reduced to R -contamination uncertainty set (9). Therefore, the proposed uncertainty set is the elaboration of the existing one (9) in a more practical way.

We conduct a theoretical analysis to derive the finite-time error bound of the proposed ARQ-Learning. Our analysis is some extension of the prior work in [6] to fit to the proposed uncertainty set. Before stating the main result, we define the useful notations and assumption. Let μ_{π_b} be the stationary distribution over $\mathcal{S} \times \mathcal{A}$ induced by behavior policy π_b . Given μ_{π_b} , we define

$$\mu_{\min} = \min_{(s,a) \in \mathcal{S} \times \mathcal{A}} \mu_{\pi_b}(s, a) \quad (18)$$

$$t_{\text{mix}} = \min \left\{ t : \max_{s \in \mathcal{S}, a \in \mathcal{A}} d_{\text{TV}}(\mu_{\pi_b}, p_s^a) \leq 0.25 \right\}, \quad (19)$$

where d_{TV} denotes the total variation distance.

Assumption 1. The Markov chain induced by the stationary behavior policy π_b and the state transition kernel $\bar{p}_s^a, \forall (s, a) \in \mathcal{S} \times \mathcal{A}$ is uniformly ergodic.

This assumption is commonly used in the analysis of vanilla Q-Learning [23] and the existing robust Q-Learning in [6].

Theorem 2: Under Assumption 1, there exist some constants $c_0, c_1 > 0$ such that for any $0 < \delta < 1$ and $0 < \varepsilon \leq \frac{1}{1-\gamma}$, the proposed ARQ-Learning in Algorithm 1 with learning rate $\alpha = \frac{c_1}{\log(|\mathcal{S}||\mathcal{A}|T)} \min \left(\frac{1}{t_{\text{mix}}}, \frac{(1-\gamma)^4 \varepsilon^2}{\gamma^2} \right)$ satisfies the following bound with probability at least $1 - \delta$:

$$|Q_T(s, a) - Q^*(s, a)| \leq \varepsilon, \quad \forall (s, a) \in \mathcal{S} \times \mathcal{A},$$

provided that T satisfies

$$T \geq \frac{c_0}{\mu_{\min}} \left(\frac{1}{(1-\gamma)^5 \varepsilon^2} + \frac{t_{\text{mix}}}{(1-\gamma)} \right) \times \log \left(\frac{|\mathcal{S}||\mathcal{A}|T}{\delta} \right) \log \left(\frac{1}{(1-\gamma)^2 \varepsilon} \right).$$

Proof: The proof is provided in Appendix B. ■

From Theorem 2, we can identify that a sample size $\tilde{\mathcal{O}} \left(\frac{1}{\mu_{\min}(1-\gamma)^5 \varepsilon^2} + \frac{t_{\text{mix}}}{\mu_{\min}(1-\gamma)} \right)$ is required to guarantee an ε -accuracy. The complexity of the proposed ARQ-Learning is well-matched with those of vanilla Q-learning in [23] and robust Q-Learning in [6] while ensuring the robustness to practical model uncertainties. Despite its effectiveness, ARQ-Learning can suffer from the large memory space to store the ITM **B** especially when the size of \mathcal{S} becomes large. We address this problem in the subsequent section by introducing the so-called pessimistic agent. The role of this agent is to

Algorithm 2 PRQ-Learning

```

1: Input: Learning rate  $\alpha > 0$ , discounted factor  $\gamma \in (0, 1)$ ,
   and robustness-level  $R$ .
2: Initialization:  $Q^\pi(\cdot, \cdot), Q^\phi(\cdot, \cdot), s_0 \in \mathcal{S}$ .
3: for each epoch do
4:   for each environment step do
5:      $x_t \leftarrow s_t, a_t \sim \pi(s_t)$ , and  $u_t \sim \phi(x_t)$ 
6:      $s_{t+1} \sim \bar{p}_{s_t}^{a_t}$  and  $x_{t+1} \sim \bar{p}_{x_t}^{u_t}$ 
7:      $c_t = c(s_t, a_t)$  and  $c_t^p = -c(x_t, u_t)$ 
8:      $\mathcal{D} \leftarrow \mathcal{D} \cup \{(s_t, a_t, c_t, s_{t+1}, u_t, c_t^p, x_{t+1})\}$ 
9:      $s_t \leftarrow s_{t+1}$ 
10:   end for
11:   for each update step do
12:      $(s, a, c, s', u, c^p, x') \sim \mathcal{D}$ 
13:      $V_t^\pi(x') = \min_{a' \in \mathcal{A}} Q_t^\pi(x', a')$ 
14:      $V_t^\pi(s') = \min_{a' \in \mathcal{A}} Q_t^\pi(s', a')$ 
15:      $V_t^\phi(x') = \min_{u' \in \mathcal{A}} Q_t^\phi(x', u')$ 
16:     Update  $Q^\phi$  via (21) and  $Q^\pi$  via (22)
17:   end for
18: end for

```

efficiently solve the maximization in (16) without estimating the ITM **B**.

B. PRQ-Learning

Despite its superiority, ARQ-Learning is not practical when the size of state space \mathcal{S} is large. To address this problem, we present an alternative approach to solve the maximization in (14) without explicitly identifying neighboring sets (i.e., without estimating the ITM **B**). Toward this, we introduce an additional agent (named pessimistic agent) whose objective is to provide the solution of the maximization in (14) (i.e., max-solver). Also, pessimistic agent can be trained only using data samples from the training environment. Both robust (or original) and pessimistic agents can be trained simultaneously although their purposes are totally different.

Pessimistic Agent. This agent aims at solving the maximization in (14) efficiently. From the cost function of robust agent $c(s, a)$, the reward function of pessimistic agent is simply defined as $c^p(s, a) = -c(s, a)$. Also, we let ϕ denote the policy of pessimistic agent. For the training of pessimistic agent, the value functions of a policy ϕ are defined as

$$V^\phi(s) = \mathbb{E}_{\phi, \mathbf{P}} \left[\sum_{t=0}^{\infty} \gamma^t c^p(s_t, a_t) \middle| s_0 = s \right]$$

$$Q^\phi(s, a) = \mathbb{E}_{\phi, \mathbf{P}} \left[\sum_{t=0}^{\infty} \gamma^t c^p(s_t, a_t) \middle| s_0 = s, a_0 = a \right].$$

Then, the optimal policy of pessimistic agent is derived as

$$\phi^* = \underset{\phi}{\operatorname{argmin}} V^\phi(s), \quad \forall s \in \mathcal{S}. \quad (20)$$

In order to distinguish from the state and action of robust agent, we let $x_t \in \mathcal{S}$ and $u_t \in \mathcal{A}$ be the state and action of pessimistic agent at time step t . Leveraging the sample

$(x_t, u_t, c_t^p = c^p(x_t, u_t), x_{t+1})$, the Q-Learning update for pessimistic agent is derived as follows:

$$Q_{t+1}^\phi(x_t, u_t) \leftarrow (1 - \alpha)Q_t^\phi(x_t, u_t) + \alpha \left(c_t^p + V_t^\phi(x_{t+1}) \right), \quad (21)$$

where $\alpha > 0$ is a learning rate. Clearly, this update is equivalent to that of vanilla Q-Learning except for cost function. However, via numerous experiments, we identify that the training of pessimistic agent suffers from being lack of exploration. We address this problem using the *state-sharing technique* (see Remark 3 for details). It is noticeable that the devise of pessimistic agent enables to extend robust RL with the proposed uncertainty set into continuous state/action spaces.

Remark 3: Pessimistic agent aims at maximizing the cumulative cost as the opposite of robust agent. As manifested in RL, the maximum cost tends to terminate an episode early, thereby hindering pessimistic agent from exploring states sufficiently, which was also confirmed via our experiments. This makes pessimistic agent to be poorly trained. We address this problem by means of the *state-sharing* technique, wherein the current state of pessimistic agent is coupled with that of robust agent. Harnessing the exploration ability of robust agent, pessimistic agent can be trained in the following ways: at every time step, before interacting with the training environment, the current state of pessimistic agent is updated as that of robust agent, i.e., $x_t = s_t$. Because of this state-sharing, in (21), the current state x_t is replaced with s_t . The details of this training are described in Algorithm 2.

Robust Agent. At every time step t , the tuple $(s_t, a_t, c_t, s_{t+1}, u_t, c_t^p, x_{t+1})$ is sampled, where $x_t = s_t$ via the state-sharing. By construction, the action of pessimistic agent u_t is sampled so that the corresponding next state x_{t+1} is likely to solve the maximization in (14) directly, i.e., $\max_{s' \in \mathcal{N}_{s_t}} V^\pi(s') \approx V^\pi(x_{t+1})$. This is verified via experiments in Section VI. Now, we tackled the most challenging part of the robust Bellman operator in (14) only using data samples from the training environment. Then, the Q-Learning update for robust agent is derived as follows:

$$Q_{t+1}^\pi(s_t, a_t) \leftarrow (1 - \alpha)Q_t^\pi(s_t, a_t) + \alpha(c_t + \gamma R \cdot V_t^\pi(x_{t+1}) + \gamma(1 - R)V_t^\pi(s_{t+1})), \quad (22)$$

where x_{t+1} is provided by pessimistic agent.

Leveraging the updates in (21) and (22), we construct **Pessimistic Robust Q-Learning (PRQ-Learning)** in Algorithm 2. One might concern that when training is premature, pessimistic agent cannot give an exact solution of the maximization in (14), i.e., $V^\pi(x_{t+1}) < \max_{s' \in \mathcal{N}_{s_t}} V^\pi(s')$. Nevertheless, it is at least guaranteed that pessimistic agent yields the state value of a certain neighboring state, i.e., $V^\pi(x_{t+1}) = V^\pi(s)$ for some $s \in \mathcal{N}_{s_t}$, thereby providing more precise value than $\max_{s' \in \mathcal{S}} V_t^\pi(s')$ in (17). As the training proceeds, furthermore, pessimistic agents tends to give an action that can lead to the solution of the maximization $\max_{s' \in \mathcal{N}_{s_t}} V^\pi(s')$. It is remarkable that the proposed PRQ-Learning can perform only using data samples from the

training environment, whereas the existing methods in [6]–[9] require some additional hard computations.

Algorithm 3 PR-DQN

```

1: Input: Learning rate  $\lambda_Q > 0$ , discounted factor  $\gamma \in (0, 1)$ ,
   robustness-level  $R$ , and  $\tau > 0$ .
2: Initialization:  $\psi, \bar{\psi}, \omega, \bar{\omega}, s_0 \in \mathcal{S}$ .
3: for each epoch do
4:   for each environment step do
5:      $x_t \leftarrow s_t$ 
6:      $a_t \sim \pi(s_t), u_t \sim \phi(x_t), s_{t+1} \sim \bar{p}_{s_t}^{a_t}$ 
7:      $x_{t+1} \sim \bar{p}_{x_t}^{u_t}$ 
8:      $c_t = c(s_t, a_t)$  and  $c_t^p = -c(x_t, u_t)$ 
9:      $\mathcal{D} \leftarrow \mathcal{D} \cup \{(s_t, a_t, c_t, s_{t+1}, u_t, c_t^p, x_{t+1})\}$ 
10:     $s_t \leftarrow s_{t+1}$ 
11:   end for
12:   for each update step do
13:      $(s, a, c, s', u, c^p, x') \sim \mathcal{D}$ 
14:      $\bar{V}^\pi(x') = \min_{a' \in \mathcal{A}} \bar{Q}^\pi(x', a')$ 
15:      $\bar{V}^\pi(s') = \min_{a' \in \mathcal{A}} \bar{Q}^\pi(s', a')$ 
16:      $\bar{V}^\phi(x') = \min_{u' \in \mathcal{A}} \bar{Q}^\phi(x', u')$ 
17:      $\psi \leftarrow \psi - \lambda_Q \nabla_{\psi} J_{Q^\phi}(\psi)$ 
18:      $\omega \leftarrow \omega - \lambda_Q \nabla_{\omega} J_{Q^\pi}(\omega)$ 
19:      $\bar{\psi} \leftarrow \tau \psi + (1 - \tau) \bar{\psi}$ 
20:      $\bar{\omega} \leftarrow \tau \omega + (1 - \tau) \bar{\omega}$ 
21:   end for
22: end for
```

V. PROPOSED FUNCTION APPROXIMATION METHODS

In this section, we extend the proposed PRQ-Learning into more practical cases that state and action spaces are larger or even continuous. This extension is made by appropriately incorporating the idea of pessimistic agent into the popular function-approximation (FA) methods such as deep-Q network (DQN) [24] and deep deterministic policy gradient (DDPG) [25]. The resulting methods are named **Pessimistic Robust DQN (PR-DQN)** and **Pessimistic Robust DDPG (PR-DDPG)**, respectively. The detailed procedures of PR-DQN and PR-DDPG are provided in Algorithm 3 and Algorithm 4, respectively. Following the notations of PRQ-Learning in Section IV-B, let s and a denote the state and action of robust agent, respectively. Also, let x and u denote the state and action of pessimistic agent, respectively. Due to the use of state-sharing technique, the tuple $(s = x, a, c, s', u, c^p, x')$ is sampled from the replay buffer.

A. PR-DQN

We propose PR-DQN by incorporating the idea of pessimistic agent in Section IV-B into DQN. In this algorithm, we define two Q-networks, named robust Q-network and pessimistic Q-network for robust and pessimistic agents, respectively. The loss function of the pessimistic Q-network (denoted by $Q^\phi(x, u; \psi)$) is defined as follows:

$$L_{Q^\phi}(\psi) = \mathbb{E}_{(x, u, c^p, x') \sim \mathcal{D}} [(Q^\phi(x, u; \psi) - y)^2], \quad (23)$$

where $y = c^p + \gamma \bar{V}^\phi(x')$ and \bar{V}^ϕ is a target network. Also, the loss function of robust Q-network (denoted by $Q^\pi(s, a; \omega)$) is defined as follows:

$$L_{Q^\pi}(\omega) = \mathbb{E}_{(s,a,c,s',x') \sim \mathcal{D}} [(Q^\pi(s, a; \omega) - y)^2], \quad (24)$$

where $y = c + \gamma(R\bar{V}^\pi(x') + (1 - R)\bar{V}^\pi(s'))$ and \bar{V}^π is a target network. The updates for the target networks \bar{V}^ϕ and \bar{V}^π are described in Algorithm 3. Like PRQ-Learning, the Q-networks are trained only using the samples from the training environment.

Algorithm 4 PR-DDPG

```

1: Input: Learning rate  $\lambda_Q > 0$ ,  $\lambda_p > 0$ , discounted factor
    $\gamma \in (0, 1)$ , robustness-level  $R$ , and  $\tau > 0$ .
2: Initialization:  $\theta, \bar{\theta}, \sigma, \bar{\sigma}, \psi, \bar{\psi}, \omega, \bar{\omega}, s_0 \in \mathcal{S}$ .
3: for each epoch do
4:   for each environment step do
5:      $x_t \leftarrow s_t$ 
6:      $a_t \sim \pi(s_t)$ ,  $u_t \sim \phi(x_t)$ ,  $s_{t+1} \sim \bar{p}_{s_t}^{a_t}$ 
7:      $x_{t+1} \sim \bar{p}_{x_t}^{u_t}$ 
8:      $c_t = c(s_t, a_t)$  and  $c_t^p = -c(x_t, u_t)$ 
9:      $\mathcal{D} \leftarrow \mathcal{D} \cup \{(s_t, a_t, c_t, s_{t+1}, u_t, c_t^p)\}$ 
10:     $s_t \leftarrow s_{t+1}$ 
11:   end for
12:   for each update step do
13:      $(s, a, c, s', u, c^p, x') \sim \mathcal{D}$ 
14:      $a'_1 \sim \bar{\pi}(s')$ ,  $a'_2 \sim \bar{\pi}(x')$  and  $u' \sim \bar{\phi}(x')$ 
15:      $\bar{V}^\pi(x') = \bar{Q}^\pi(x', a'_2)$ 
16:      $\bar{V}^\pi(s') = \bar{Q}^\pi(s', a'_1)$ 
17:      $\bar{V}^\phi(x') = \bar{Q}^\phi(x', u')$ 
18:      $\psi \leftarrow \psi - \lambda_Q \nabla_\psi J_{Q^\phi}(\psi)$ 
19:      $\omega \leftarrow \omega - \lambda_Q \nabla_\omega J_{Q^\pi}(\omega)$ 
20:      $\sigma \leftarrow \sigma - \lambda_p \nabla_\sigma J_\phi(\sigma)$ 
21:      $\theta \leftarrow \theta - \lambda_p \nabla_\theta J_\pi(\theta)$ 
22:      $\bar{\psi} \leftarrow \tau\psi + (1 - \tau)\bar{\psi}$ 
23:      $\bar{\omega} \leftarrow \tau\omega + (1 - \tau)\bar{\omega}$ 
24:      $\bar{\theta} \leftarrow \tau\theta + (1 - \tau)\bar{\theta}$ 
25:      $\bar{\sigma} \leftarrow \tau\sigma + (1 - \tau)\bar{\sigma}$ 
26:   end for
27: end for

```

B. PR-DDPG

We propose PR-DDPG by incorporating the idea of pessimistic agent in Section IV-B into DDPG. In this algorithm, we define the four DNNs such as $Q^\pi(s, a; \omega)$ and $\pi(s; \theta)$ for robust agent and $Q^\phi(x, u; \psi)$ and $\phi(x; \sigma)$ for pessimistic agent. Compared with PR-DQN, policy functions for continuous action space are additionally defined via DNNs. Thus, during the training, the parameters ω, θ, ψ , and σ should be learned simultaneously. In PR-DDPG, the loss functions for Q-networks are exactly same as PR-DQN and thus, we use the loss functions in (23) for Q^ϕ and (24) for Q^π , respectively. We only need to provide the loss functions for policy networks. The loss function of the policy-network for pessimistic agent (denoted by $\phi(x; \sigma)$) is defined as

$$L_\phi(\sigma) = \mathbb{E}_{x \sim \mathcal{D}} [Q^\phi(x, u; \psi) |_{u=\phi(x; \sigma)}]. \quad (25)$$

TABLE I
HYPER-PARAMETERS FOR TABULAR ALGORITHMS

	FrozenLake-v1	CliffWalking-v0
γ	0.99	0.99
α	0.01	0.01
Batch Size	32	32
Buffer Size	20000	20000
Max Episode times	4000	1000

Also, the loss function of the policy-network for robust agent (denoted by $\pi(s; \theta)$) is defined as

$$L_\pi(\theta) = \mathbb{E}_{s \sim \mathcal{D}} [Q^\pi(s, a; \omega) |_{a=\pi(s; \theta)}]. \quad (26)$$

Both loss functions are the same as vanilla DDPG [25]. However, since Q-networks are trained according to the robust Bellman operator in (14), robust agent in PR-DDPG is able to learn a robust action compared with vanilla DDPG.

Remark 4: While we used DQN and DDPG as the baseline RL algorithms, one can easily incorporate the idea of pessimistic agent into the other model-free RL algorithms (e.g., SAC [26] TD3 [27] and PPO [28]). Specifically, the value function of robust agent is trained using the modified loss function according to the robust Bellman operator in (14). Also, pessimistic agent can be trained in the same way as PR-DQN in discrete action space or PR-DDPG in continuous action space.

VI. EXPERIMENTS

In this section, we conduct the experiments to validate the superiority of our algorithms such as ARQ-Learning, PRQ-Learning, DQN-Learning, and DDPG-Learning. For comparisons, the following benchmark algorithms are considered:

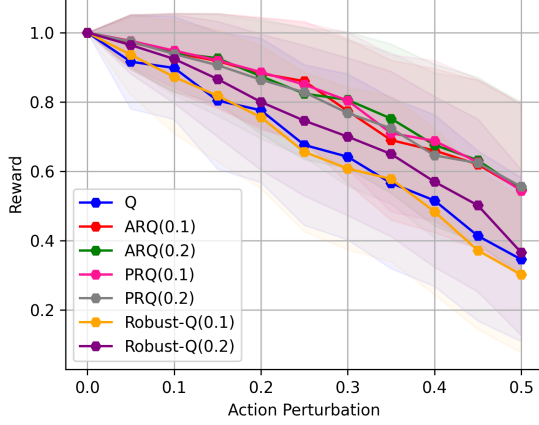
- The popular RL algorithms such as Q-Learning [1], DQN [24], and DDPG [25] as they are used as the baseline methods of the proposed algorithms.
- The state-of-the-art robust RL algorithms such as robust Q-Learning (in short, Robust-Q) [6] for tabular case.
- To the best of our knowledge, there is no efficient robust RL algorithms for continuous state spaces. In [6], robust Q-Learning was only extended with a simple linear function approximation. Thus, based on DNNs, we implemented Robust-DQN and Robust-DDPG (in short, R-DQN and R-DDPG) by appropriately combining DQN and DDPG with R -contamination uncertainty set [6]. As aforementioned, it is hard to find the maximum in (17) exactly as an entire state space must be searched. To overcome this, we stored action values in an additional buffer during training and estimated the maximum of value function in (17) by taking the maximum among the stored values in the buffer.

OpenAI gym [29] is used for various environments.

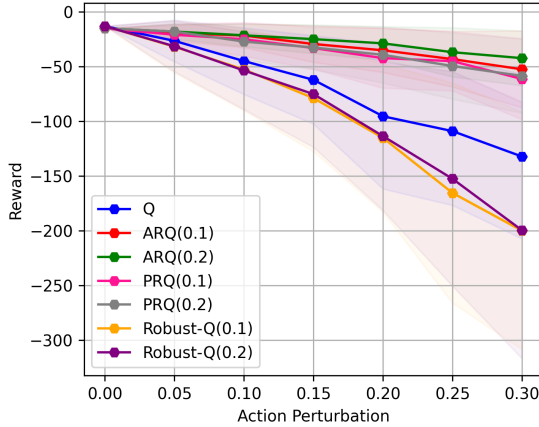
In our experiments, an agent is trained from training environment (i.e., N-MDP) and then, our learned agent is evaluated from testing environment. To evaluate the robustness, there is some mismatches between testing and training environments.

TABLE II
HYPER-PARAMETERS FOR FUNCTION APPROXIMATION ALGORITHMS

	Acrobot-v1	CartPole-v1	MountainCar-v0	Pendulum-v1
Hidden Layers	[64, 64]	[64, 64]	[64, 64]	[256, 256]
γ	0.99	0.99	0.99	0.99
τ	0.01	0.01	0.01	0.05
Batch Size	32	32	32	32
Buffer Size	20000	20000	20000	20000
Learning Rate	0.0001	0.001	0.001	0.0001(A), 0.001(C)
Max Episode times	500	1000	2000	300
Value Memory Size	32×30	32×30	32×30	32×30



(a) FrozenLake-v1(8x8)



(b) CliffWalking-v0

Fig. 2. Performance comparisons of various tabular methods under action perturbations, where FrozenLake-v1 is set as non-slippery. The values in the parenthesis indicate the robustness level R .

Among various types of perturbations (or mismatches), we take into account action and parameter perturbations. First, action-perturbation implies that an agent can take a random action with some probability, instead of solely complying the optimal policy (provided by a learned policy). This type of perturbations can occur in real-world applications. For example, when an agent's observation is different from the environment's state, an action taken from the agent might not be optimal action. In addition, it is possible that in

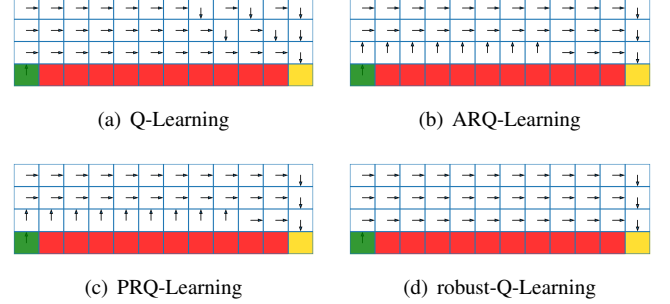


Fig. 3. The expressions of optimal actions in CliffWalking-v0, where green, red, and yellow colors denote start, cliff, and goal states, respectively.

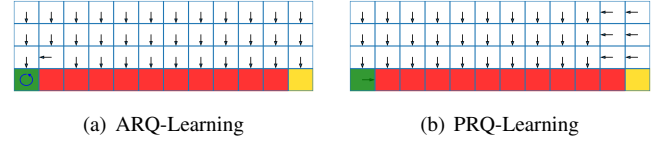
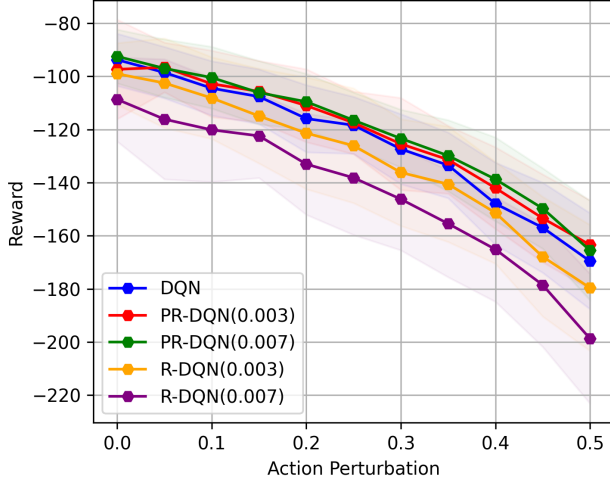


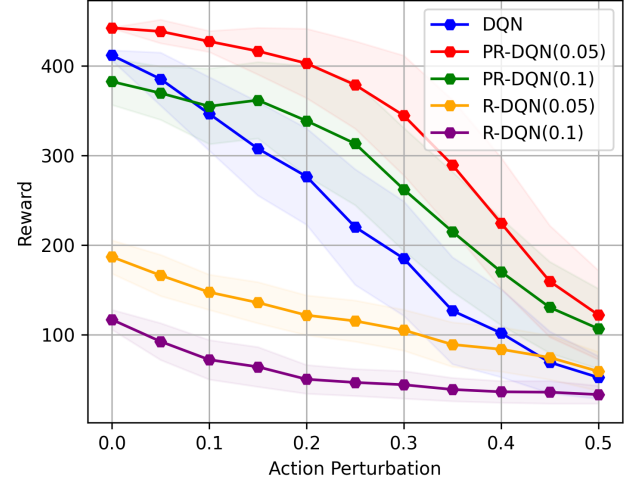
Fig. 4. The expressions of max-state $s' = \arg\max_{s' \in \mathcal{N}_s} V^\pi(s')$ provided by ARQ-Learning and PRQ-Learning in CliffWalking-v0.

the application of autonomous driving, agent's action can be performed with some noises. Specifically, a drone flying in the air may be pushed by some unexpected air-flow from any direction and with any strength. Second, parameter-perturbation implies that some parameter settings in training environment can be different from that in testing environment. This type of perturbation can well-represent the modeling mismatches between simulator model (i.e., training environment) and real-world setting (i.e., testing environment). In order to see the impact of robustness level $R > 0$, we choose two different values of R except the vanilla RL algorithms. An agent is trained with five instances for each algorithm. At evaluation time step, we take the average reward and standard deviation of 100 tests for each instance. For each figure, the thick line represents the average value and light region shows the ± 0.5 standard deviation. The hyper-parameters for the proposed and benchmark algorithms are provided in Table I and Table II, where 'A' and 'C' stand for actor and critic, respectively.

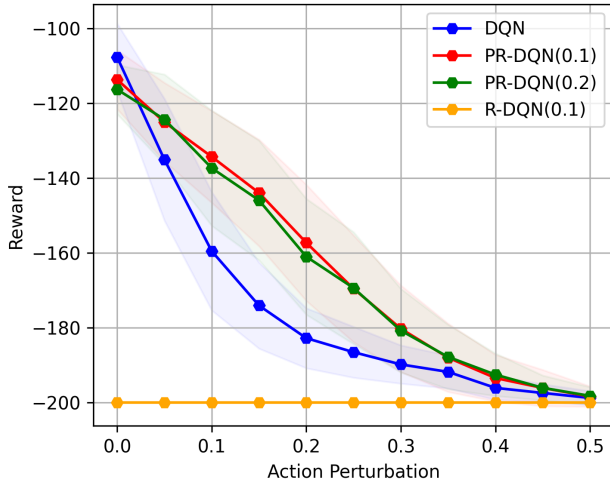
Fig. 2 shows that the proposed PRQ-Learning yields the robustness against the action perturbations, whereas the benchmark algorithms seem to have failed. We can identify the reason for the superiority of our algorithm from Fig. 3, in which red boxes denote the cliff that gives the highest cost



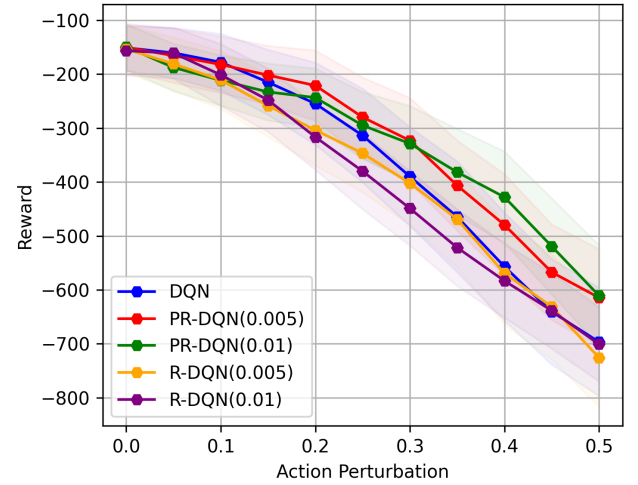
(a) Acrobot-v1



(b) CartPole-v1



(c) MountainCar-v0



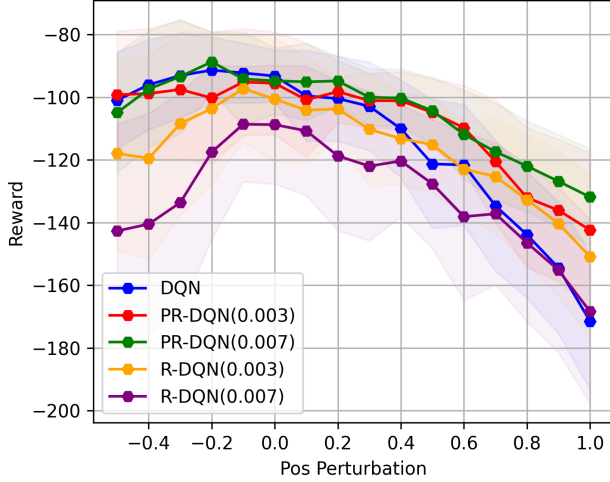
(d) Pendulum-v1

Fig. 5. Performance comparisons of various function-approximation algorithms under action perturbations. The values in the parenthesis indicate the robustness level R .

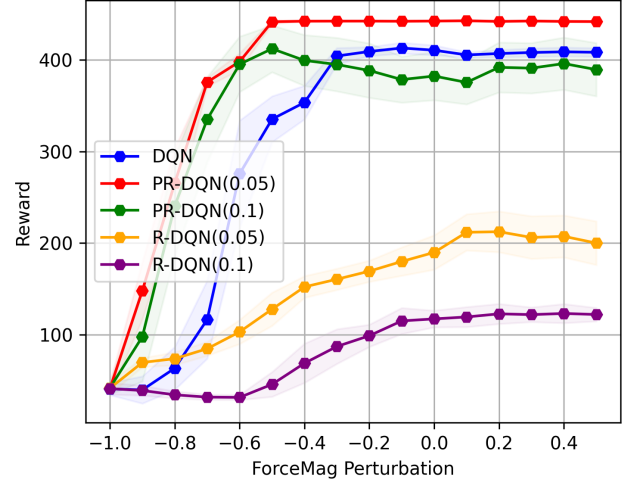
to the agent. We can observe that the agent trained with Q-Learning takes the actions so that it moves right above the cliff (i.e., the shortest path to reach the goal). On the other hand, the agents trained with ARQ- and PRQ-Learning take the actions so that they tend to choose the path far from the cliff. This indeed shows that ARQ- and PRQ-Learning can learn some potential dangers of adjacent states. Also, Fig. 4 shows the estimated maximum state $s' = \operatorname{argmax}_{s' \in \mathcal{N}_s} V^\pi(s')$ in ARQ-Learning and PRQ-Learning. This state is estimated from ITM B for ARQ-Learning and by pessimistic agent for PRQ-Learning. We can observe that the estimated states are the almost same for both algorithms. This verifies that pessimistic agent indeed solves the maximization (14). It is remarkable that the agent trained with Robust-Q is failed to learn a robust action. This is because in R -contamination uncertainty set, the agent is trained by considering the dangers of the whole states rather than those of neighboring states. In other words, this agent overestimates potential dangers in the environment,

instead of reflecting them at some particular states nearby the cliff.

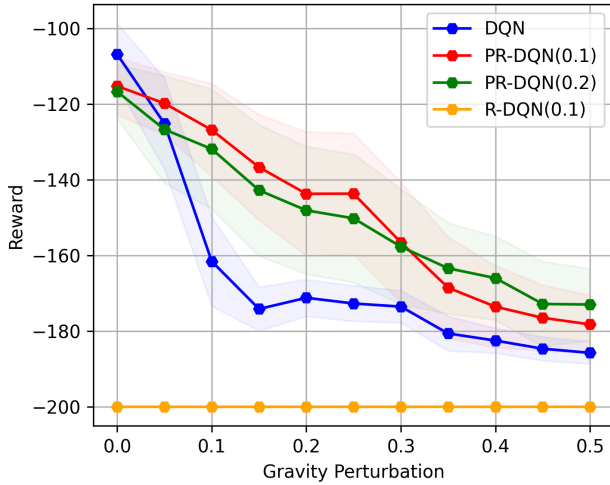
Focusing on continuous state and/or action spaces, we conduct the experiments of function-approximation algorithms. The corresponding results are provided in Figs. 5 and 6. We observe that the proposed PR-DQN and PR-DDPG achieve higher rewards than the benchmark function-approximation algorithms such as DQN, DDPG, R-DQN, and R-DDPG in the presence of action- and parameter-perturbation. Remarkably, although the proposed algorithms are trained basically against action perturbations, they can yield greater rewards in parameter-perturbation as well. There are some cases that vanilla RL algorithms achieve higher rewards than the proposed algorithms in non-perturbation situations. However, it is reasonable that in this case, training and testing environments are identical. When perturbations are applied, the proposed algorithms attain higher rewards than the vanilla ones. Like the tabular cases, the proposed algorithms outperform the



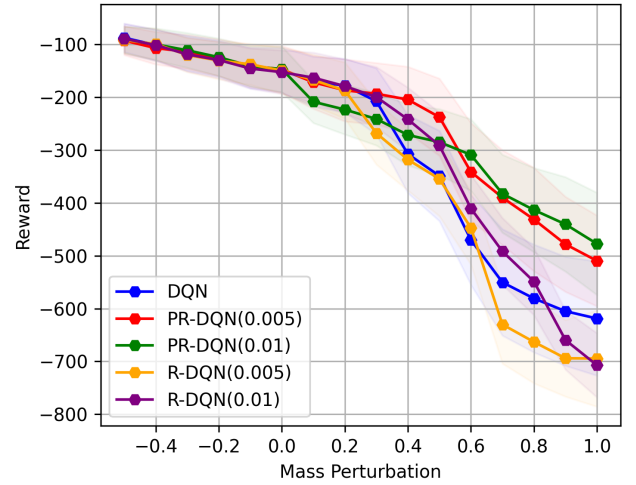
(a) Acrobot-v1



(b) CartPole-v1



(c) MountainCar-v0



(d) Pendulum-v1

Fig. 6. Performance comparisons of various function-approximation algorithms under parameter perturbations. The values in the parenthesis indicate the robustness level R .

benchmark robust algorithms such as R-DQN and R-DDPG while ensuring better robustness to the perturbations in testing environment. These results strengthen our argument that the proposed uncertainty set better reflects real-world perturbations (or uncertainties).

VII. CONCLUSION

We presented the novel uncertainty set (named adjacent R -contamination uncertainty set), which can better reflect real-world perturbations than the existing ones. Under this set, we first presented ARQ-Learning for tabular cases and theoretically characterized its performance bound. Also, it was proved that ARQ-Learning can converge to an optimal value as fast as Q-Learning and the state-of-the-art robust Q-Learning while ensuring more robustness to real-world applications. We introduced pessimistic agent, which can tackle the key bottleneck for the extension of ARQ-Learning into continuous state spaces. Leveraging pessimistic agent, we

constructed PRQ-Learning suitable for tabular cases with large state spaces, and PR-DQN and PR-DDPG for continuous state spaces. While the proposed algorithms are based on DQN and DDPG as the baseline RL algorithms, we remark that our key idea to use the adjacent R -contamination uncertainty set and pessimistic agent can be immediately integrated with the other model-free algorithms (e.g., soft actor critic (SAC), twin delayed deep deterministic policy gradient (TD3) and proximal policy optimization (PPO)). Via experiments, we verified the superiority of our algorithms on various real-world RL applications with model mismatches. It would be an interesting future work to extend our algorithms into offline RL.

APPENDIX A PROOF OF THEOREM 1

We prove Theorem 1. In [6], it was proved that the robust Bellman operator for R -contamination uncertainty set is

contraction. In this section, we extend this to the proposed *adjacent* R -contamination uncertainty set. In the below, it is assumed that the neighboring set of a state $s \in \mathcal{S}$ at least includes s as its element $s \in \mathcal{N}_s$, to ensure that the neighboring set is not empty set (i.e., $\mathcal{N}_s \neq \emptyset$). This assumption makes sense in practice because if an agent does not take any action, it can stay at the current state with non-zero probability. First we have:

$$\begin{aligned}
& |\mathbf{T}Q_1(s, a) - \mathbf{T}Q_2(s, a)| \\
&= \left| c(s, a) + \gamma(1 - R) \left[\sum_{s' \in \mathcal{S}} \bar{p}_{s, s'}^a V_1(s') \right] + \gamma R \left[\max_{s' \in \mathcal{N}_s} V_1(s') \right] \right. \\
&\quad \left. - c(s, a) - \gamma(1 - R) \left[\sum_{s' \in \mathcal{S}} \bar{p}_{s, s'}^a V_2(s') \right] - \gamma R \left[\max_{s' \in \mathcal{N}_s} V_2(s') \right] \right| \\
&= \left| \gamma(1 - R) \left[\sum_{s' \in \mathcal{S}} \bar{p}_{s, s'}^a (V_1(s') - V_2(s')) \right] \right. \\
&\quad \left. + \gamma R \left(\max_{s' \in \mathcal{N}_s} V_1(s') - \max_{s' \in \mathcal{N}_s} V_2(s') \right) \right| \\
&\leq \left| \gamma(1 - R) \left[\sum_{s' \in \mathcal{S}} \bar{p}_{s, s'}^a \left(\min_a Q_1(s', a) - \min_a Q_2(s', a) \right) \right] \right| \\
&\quad + \left| \gamma R \max_{s' \in \mathcal{N}_s} (V_1(s') - V_2(s')) \right| \\
&\leq \gamma(1 - R) \sum_{s' \in \mathcal{S}} \bar{p}_{s, s'}^a \left| \min_a Q_1(s', a) - \min_a Q_2(s', a) \right| \\
&\quad + \gamma R \max_{s' \in \mathcal{N}_s} |V_1(s') - V_2(s')| \\
&\stackrel{(a)}{\leq} \gamma(1 - R) \|Q_1 - Q_2\|_\infty + \gamma R \|Q_1 - Q_2\|_\infty \\
&= \gamma \|Q_1 - Q_2\|_\infty,
\end{aligned} \tag{27}$$

where (a) is due to the following facts 1) and 2):

1) If $\min_a Q_1(s', a) \geq \min_a Q_2(s', a)$, then we have:

$$\begin{aligned}
& \left| \min_a Q_1(s', a) - \min_a Q_2(s', a) \right| \\
&= \min_a Q_1(s', a) - \min_a Q_2(s', a) \\
&\leq Q_1(s', b) - Q_2(s', b) \\
&\leq \|Q_1 - Q_2\|_\infty,
\end{aligned}$$

where $b = \operatorname{argmin}_a Q_2(s', a)$.

2) If $\min_a Q_1(s', a) < \min_a Q_2(s', a)$, then we have:

$$\begin{aligned}
& \left| \min_a Q_1(s', a) - \min_a Q_2(s', a) \right| \\
&= \min_a Q_2(s', a) - \min_a Q_1(s', a) \\
&\leq Q_2(s', c) - Q_1(s', c) \\
&\leq \|Q_1 - Q_2\|_\infty,
\end{aligned}$$

where $c = \operatorname{argmin}_a Q_1(s', a)$.

Also, we can obtain the following inequality:

$$\begin{aligned}
\max_{s' \in \mathcal{N}_s} |V_1(s') - V_2(s')| &\leq \max_{s' \in \mathcal{S}} |V_1(s') - V_2(s')| \\
&\leq \|Q_1 - Q_2\|_\infty.
\end{aligned} \tag{28}$$

We now proved that our robust Bellman operator \mathbf{T} is contraction with respect to l_∞ -norm. From Banach fixed point

theorem [30], we also proved that Q^π has the unique fixed point of \mathbf{T} . This completes the proof of Theorem 1.

APPENDIX B PROOF OF THEOREM 2

We prove Theorem 2. As in Appendix A, it is assumed that an estimated neighboring set $\hat{\mathcal{N}}_s$ is not empty set (i.e., $\hat{\mathcal{N}}_s \neq \emptyset$). As explained before, it is reasonable assumption in practical RL applications. We first introduce the useful vector notations. Let $V_t \in \mathbb{R}^{|\mathcal{S}|}$ and $Q_t \in \mathbb{R}^{|\mathcal{S}| \times |\mathcal{A}|}$ denote the vector representations of the estimation of value functions at time step t . Also, we let $V^* \in \mathbb{R}^{|\mathcal{S}|}$ and $Q^* \in \mathbb{R}^{|\mathcal{S}| \times |\mathcal{A}|}$ denote the vector representations of optimal value functions. Let $c \in \mathbb{R}^{|\mathcal{S}| \times |\mathcal{A}|}$ be the vector representation of the cost function such that the (s, a) -th entry of c is equal to $c(s, a)$.

Using the vector notations, given $(s, a) \in \mathcal{S} \times \mathcal{A}$, we define the transition kernel vector $P_s^a \in \mathbb{R}^{|\mathcal{S}|}$ as

$$P_s^a(s') = \bar{p}_{s, s'}^a. \tag{29}$$

Also, given a sample $O_t = (s_t, a_t, s_{t+1})$, we can define the sample transition vector $P_{s, t+1}^a \in \mathbb{R}^{|\mathcal{S}|}$ as

$$P_{s, t+1}^a(s') = \begin{cases} 1, & \text{if } (s, a, s') = O_t \\ 0, & \text{otherwise.} \end{cases} \tag{30}$$

Then, the update of ARQ-Learning at the (s, a) -th element can be rewritten as

$$\begin{aligned}
Q_t(s, a) &= (1 - \alpha \mathbb{1}_{\{s=s_t\}}) Q_{t-1}(s, a) \\
&\quad + \alpha \mathbb{1}_{\{s=s_t\}} \left(c(s, a) + \gamma(1 - R) (P_{s, t}^a)^\top V_{t-1} \right. \\
&\quad \left. + \gamma R \max_{s' \in \hat{\mathcal{N}}_{s_t}} V_{t-1}(s') \right)
\end{aligned} \tag{31}$$

$$\begin{aligned}
&= (1 - \alpha \mathbb{1}_{\{s=s_t\}}) Q_{t-1}(s, a) \\
&\quad + \alpha \mathbb{1}_{\{s=s_t\}} \left(c(s, a) + \gamma(1 - R) (P_{s, t}^a)^\top V_{t-1} \right. \\
&\quad \left. + \gamma R \max_{s' \in \hat{\mathcal{N}}_s} V_{t-1}(s') \right),
\end{aligned} \tag{32}$$

where $\mathbb{1}_{\{\cdot\}}$ represents an indicator function. Although $\hat{\mathcal{N}}_{s_t}$ and $\hat{\mathcal{N}}_s$ are different in the maximization in (31) and (32), we can easily identify that (32) is equivalent to (31) due to the indicator function $\mathbb{1}_{\{s=s_t\}}$. Also, the optimal robust Bellman equation can be expressed as

$$Q^*(s, a) = c(s, a) + \gamma(1 - R) (P_s^a)^\top V^* + \gamma R \max_{s' \in \hat{\mathcal{N}}_s} V^*(s'). \tag{33}$$

We let:

$$\psi_t(s, a) \triangleq Q_t(s, a) - Q^*(s, a). \tag{34}$$

Using this notation, we have:

$$\begin{aligned}
\psi_t(s, a) &= Q_t(s, a) - Q^*(s, a) \\
&= (1 - \alpha \mathbb{1}_{\{s=s_t\}}) (Q_{t-1}(s, a) - Q^*(s, a)) \\
&\quad + \alpha \mathbb{1}_{\{s=s_t\}} (Q_t(s, a) - Q^*(s, a)) \\
&= (1 - \alpha \mathbb{1}_{\{s=s_t\}}) \psi_{t-1}(s, a) \\
&\quad + \alpha \mathbb{1}_{\{s=s_t\}} \gamma (1 - R) ((P_{s,t}^a)^\top V_{t-1} - (P_s^a)^\top V^*) \\
&\quad + \alpha \mathbb{1}_{\{s=s_t\}} \gamma R \left(\max_{s \in \tilde{\mathcal{N}}_s} V_{t-1}(s) - \max_{s \in \tilde{\mathcal{N}}_s} V^*(s) \right) \\
&= (1 - \alpha \mathbb{1}_{\{s=s_t\}}) \psi_{t-1}(s, a) \\
&\quad + \alpha \gamma (1 - R) \mathbb{1}_{\{s=s_t\}} ((P_{s,t}^a)^\top V_{t-1} - (P_{s,t}^a)^\top V^*) \\
&\quad + \alpha \gamma (1 - R) \mathbb{1}_{\{s=s_t\}} ((P_{s,t}^a)^\top V^* - (P_s^a)^\top V^*) \\
&\quad + \alpha \gamma R \mathbb{1}_{\{s=s_t\}} \left(\max_{s \in \tilde{\mathcal{N}}_s} V_{t-1}(s) - \max_{s \in \tilde{\mathcal{N}}_s} V^*(s) \right) \\
&= (1 - \alpha \mathbb{1}_{\{s=s_t\}}) \psi_{t-1}(s, a) \\
&\quad + \alpha \gamma (1 - R) \mathbb{1}_{\{s=s_t\}} (P_{s,t}^a - P_s^a)^\top V^* \\
&\quad + \alpha \gamma (1 - R) \mathbb{1}_{\{s=s_t\}} (P_{s,t}^a)^\top (V_{t-1} - V^*) \\
&\quad + \alpha \gamma R \mathbb{1}_{\{s=s_t\}} \left(\max_{s \in \tilde{\mathcal{N}}_s} V_{t-1}(s) - \max_{s \in \tilde{\mathcal{N}}_s} V^*(s) \right).
\end{aligned}$$

Applying this relation recursively, we can get:

$$\psi_t(s, a) = \beta_{1,t}(s, a) + \beta_{2,t}(s, a) + \beta_{3,t}(s, a), \quad (35)$$

where $\beta_{1,t}(s, a)$, $\beta_{2,t}(s, a)$, and $\beta_{3,t}(s, a)$ are respectively defined as

$$\beta_{1,t}(s, a) = \prod_{j=1}^t (1 - \mathbb{1}_{\{s=s_j\}}) \psi_0(s, a) \quad (36)$$

$$\begin{aligned}
\beta_{2,t}(s, a) &= \gamma (1 - R) \sum_{i=1}^t \prod_{j=i+1}^t (1 - \mathbb{1}_{\{s=s_j\}}) \mathbb{1}_{\{s=s_i\}} \\
&\quad \times (P_{s,i}^a - P_s^a)^\top V^* \quad (37)
\end{aligned}$$

$$\begin{aligned}
\beta_{3,t}(s, a) &= \gamma (1 - R) \sum_{i=1}^t \prod_{j=i+1}^t (1 - \mathbb{1}_{\{s=s_j\}}) \mathbb{1}_{\{s=s_i\}} \\
&\quad \times (P_{s,i}^a)^\top (V_{i-1} - V^*) \\
&\quad + \gamma R \sum_{i=1}^t \prod_{j=i+1}^t (1 - \mathbb{1}_{\{s=s_j\}}) \mathbb{1}_{\{s=s_i\}} \\
&\quad \times \left(\max_{s \in \tilde{\mathcal{N}}_s} V_{i-1}(s) - \max_{s \in \tilde{\mathcal{N}}_s} V^*(s) \right). \quad (38)
\end{aligned}$$

Applying the triangle inequality to (B), we can obtain the upper bound of $\psi_t(s, a)$ such as

$$|\psi_t(s, a)| \leq |\beta_{1,t}(s, a)| + |\beta_{2,t}(s, a)| + |\beta_{3,t}(s, a)|. \quad (39)$$

In Lemmas 1, 2, and 3 below, we derive the upper bounds of $\beta_{1,t}(s, a)$, $\beta_{2,t}(s, a)$, and $\beta_{3,t}(s, a)$, respectively. Combining them, we can obtain the upper bound of $\psi_t(s, a)$ as follows:

- For $t < t_{\text{frame}}$, we have:

$$\begin{aligned}
|\psi_t(s, a)| &\leq \|\psi_0\|_\infty + \gamma c \sqrt{\alpha \log \frac{|\mathcal{S}||\mathcal{A}|T}{\delta}} \|V^*\|_\infty \\
&\quad + \gamma \sum_{i=1}^t \|\psi_{i-1}\|_\infty \prod_{j=i+1}^t (1 - \mathbb{1}_{\{s=s_j\}}) \mathbb{1}_{\{s=s_i\}}.
\end{aligned}$$

- For $t_{\text{frame}} \leq t \leq T$, we have:

$$\begin{aligned}
|\psi_t(s, a)| &\leq (1 - \alpha)^{\frac{t\mu_{\min}}{2}} \|\psi_0\|_\infty \\
&\quad + \gamma c \sqrt{\alpha \log \frac{|\mathcal{S}||\mathcal{A}|T}{\delta}} \|V^*\|_\infty \\
&\quad + \gamma \sum_{i=1}^t \|\psi_{i-1}\|_\infty \prod_{j=i+1}^t (1 - \mathbb{1}_{\{s=s_j\}}) \mathbb{1}_{\{s=s_i\}}.
\end{aligned}$$

This bound exactly matches the bound in the Equation (42) in [23]. Thus, the remaining of Theorem 2 can be obtained by exactly following the proof of [23, Theorem 5]. This completes the proof of Theorem 2.

Lemma 1: For any $\delta > 0$ and $t_{\text{frame}} = \frac{443t_{\text{mix}}}{\mu_{\min}} \log \left(\frac{4|\mathcal{S}||\mathcal{A}|T}{\delta} \right)$ with $t_{\text{frame}} \leq T$, with probability at least $1 - \delta$, $\beta_{1,t}(s, a)$ is bounded as

$$|\beta_{1,t}(s, a)| \leq \begin{cases} (1 - \alpha)^{\frac{1}{2}t\mu_{\min}} \|\psi_0\|_\infty, & t_{\text{frame}} < \forall t < T \\ |\beta_{1,t}(s, a)| \leq \|\psi_0\|_\infty, & \forall t < t_{\text{frame}}. \end{cases}$$

Proof: The proof exactly follows the proof of [23, Lemma 2]. ■

Lemma 2: There exists some constant $c > 0$ such that for any $0 < \delta < 1$ and $t \leq T$ that satisfies $0 < \alpha \log \frac{|\mathcal{S}||\mathcal{A}|T}{\delta} < 1$, with probability at least $1 - \delta$, we have that for $\forall (s, a) \in \mathcal{S} \times \mathcal{A}$,

$$\begin{aligned}
|\beta_{2,t}(s, a)| &\leq c\gamma(1 - R) \sqrt{\eta \log \left(\frac{|\mathcal{S}||\mathcal{A}|T}{\delta} \right)} \|V^*\|_\infty \\
&\leq c\gamma \sqrt{\eta \log \left(\frac{|\mathcal{S}||\mathcal{A}|T}{\delta} \right)} \|V^*\|_\infty.
\end{aligned}$$

Proof: The proof exactly follows the proof of [23, Lemma 1]. ■

Lemma 3: For any $t > 0$, we have that for $\forall (s, a) \in \mathcal{S} \times \mathcal{A}$,

$$|\beta_{3,t}(s, a)| \leq \gamma \sum_{i=1}^t \|\psi_{i-1}\|_\infty \prod_{j=i+1}^t (1 - \mathbb{1}_{\{s=s_j\}}) \mathbb{1}_{\{s=s_i\}}.$$

Proof: We first have:

$$\begin{aligned}
|(P_{s,i}^a)^\top (V_{i-1} - V^*)| &\leq \|P_{s,i}^a\|_\infty \|V_{i-1} - V^*\|_\infty \\
&\leq \|V_{i-1} - V^*\|_\infty \\
&= \max_s |V_{i-1}(s) - V^*(s)| \\
&= |V_{i-1}(s^*) - V^*(s^*)| \\
&= \left| \min_a Q_{i-1}(s^*, a) - \min_b Q^*(s^*, b) \right| \\
&\leq \|Q_{i-1} - Q^*\|_\infty \\
&= \|\psi_{i-1}\|_\infty, \quad (40)
\end{aligned}$$

where $s^* = \arg \max_{s \in \mathcal{S}} |V_{i-1}(s) - V^*(s)|$. Also, we can get:

$$\begin{aligned}
\left| \max_{s \in \tilde{\mathcal{N}}_s} V_{i-1}(s) - \max_{s \in \tilde{\mathcal{N}}_s} V^*(s) \right| &\leq \|V_{i-1} - V^*\|_\infty \\
&\leq \|Q_{i-1} - Q^*\|_\infty \\
&= \|\psi_{i-1}\|_\infty. \quad (41)
\end{aligned}$$

It is obvious that $0 \leq (1 - \mathbb{1}_{s=s'}) \leq 1$ and $0 \leq \mathbb{1}_{s=s'} \leq 1$ for $\forall s, s' \in \mathcal{S}$. Thus, we have:

$$|\beta_{3,t}(s, a)| \leq \gamma \sum_{i=1}^t \|\psi_{t-1}\|_{\infty} \prod_{j=i+1}^t (1 - \mathbb{1}_{\{s=s_j\}}) \mathbb{1}_{\{s=s_i\}}.$$

This completes the proof of Lemma 3. \blacksquare

REFERENCES

- [1] R. S. Sutton and A. G. Barto, *Reinforcement learning: An introduction*. MIT press, 2018.
- [2] C. Szepesvári, “Algorithms for reinforcement learning,” *Synthesis lectures on artificial intelligence and machine learning*, vol. 4, no. 1, pp. 1–103, 2010.
- [3] J. A. Bagnell, A. Y. Ng, and J. G. Schneider, “Solving uncertain markov decision processes,” 2001.
- [4] A. Nilim and L. Ghaoui, “Robustness in markov decision problems with uncertain transition matrices,” *Advances in neural information processing systems*, vol. 16, 2003.
- [5] G. N. Iyengar, “Robust dynamic programming,” *Mathematics of Operations Research*, vol. 30, no. 2, pp. 257–280, 2005.
- [6] Y. Wang and S. Zou, “Online robust reinforcement learning with model uncertainty,” *Advances in Neural Information Processing Systems*, vol. 34, pp. 7193–7206, 2021.
- [7] Y. Wang and S. Zou, “Policy gradient method for robust reinforcement learning,” in *International Conference on Machine Learning*, pp. 23484–23526, PMLR, 2022.
- [8] K. P. Badrinath and D. Kalathil, “Robust reinforcement learning using least squares policy iteration with provable performance guarantees,” in *International Conference on Machine Learning*, pp. 511–520, PMLR, 2021.
- [9] A. Roy, H. Xu, and S. Pokutta, “Reinforcement learning under model mismatch,” *Advances in neural information processing systems*, vol. 30, 2017.
- [10] A. Nilim and L. El Ghaoui, “Robust control of markov decision processes with uncertain transition matrices,” *Operations Research*, vol. 53, no. 5, pp. 780–798, 2005.
- [11] W. Wiesemann, D. Kuhn, and B. Rustem, “Robust markov decision processes,” *Mathematics of Operations Research*, vol. 38, no. 1, pp. 153–183, 2013.
- [12] A. Tamar, S. Mannor, and H. Xu, “Scaling up robust mdps using function approximation,” in *International conference on machine learning*, pp. 181–189, PMLR, 2014.
- [13] A. Rajeswaran, S. Ghotra, B. Ravindran, and S. Levine, “Epopt: Learning robust neural network policies using model ensembles,” *arXiv preprint arXiv:1610.01283*, 2016.
- [14] L. Pinto, J. Davidson, R. Sukthankar, and A. Gupta, “Robust adversarial reinforcement learning,” in *International Conference on Machine Learning*, pp. 2817–2826, PMLR, 2017.
- [15] M. A. Abdullah, H. Ren, H. B. Ammar, V. Milenkovic, R. Luo, M. Zhang, and J. Wang, “Wasserstein robust reinforcement learning,” *arXiv preprint arXiv:1907.13196*, 2019.
- [16] E. Vinitsky, Y. Du, K. Parvate, K. Jang, P. Abbeel, and A. Bayen, “Robust reinforcement learning using adversarial populations,” *arXiv preprint arXiv:2008.01825*, 2020.
- [17] L. Hou, L. Pang, X. Hong, Y. Lan, Z. Ma, and D. Yin, “Robust reinforcement learning with wasserstein constraint,” *arXiv preprint arXiv:2006.00945*, 2020.
- [18] S. Huang, N. Papernot, I. Goodfellow, Y. Duan, and P. Abbeel, “Adversarial attacks on neural network policies,” *arXiv preprint arXiv:1702.02284*, 2017.
- [19] J. Kos and D. Song, “Delving into adversarial attacks on deep policies,” *arXiv preprint arXiv:1705.06452*, 2017.
- [20] A. Pattanaik, Z. Tang, S. Liu, G. Bommannan, and G. Chowdhary, “Robust deep reinforcement learning with adversarial attacks,” *arXiv preprint arXiv:1712.03632*, 2017.
- [21] A. Mandelkar, Y. Zhu, A. Garg, L. Fei-Fei, and S. Savarese, “Adversarially robust policy learning: Active construction of physically-plausible perturbations,” in *2017 IEEE/RSJ International Conference on Intelligent Robots and Systems (IROS)*, pp. 3932–3939, IEEE, 2017.
- [22] P. J. Huber, “A robust version of the probability ratio test,” *The Annals of Mathematical Statistics*, pp. 1753–1758, 1965.
- [23] G. Li, Y. Wei, Y. Chi, Y. Gu, and Y. Chen, “Sample complexity of asynchronous q-learning: Sharper analysis and variance reduction,” *Advances in neural information processing systems*, vol. 33, pp. 7031–7043, 2020.
- [24] V. Mnih, K. Kavukcuoglu, D. Silver, A. A. Rusu, J. Veness, M. G. Bellemare, A. Graves, M. Riedmiller, A. K. Fidjeland, G. Ostrovski, et al., “Human-level control through deep reinforcement learning,” *nature*, vol. 518, no. 7540, pp. 529–533, 2015.
- [25] T. P. Lillicrap, J. J. Hunt, A. Pritzel, N. Heess, T. Erez, Y. Tassa, D. Silver, and D. Wierstra, “Continuous control with deep reinforcement learning,” *arXiv preprint arXiv:1509.02971*, 2015.
- [26] T. Haarnoja, A. Zhou, P. Abbeel, and S. Levine, “Soft actor-critic: Off-policy maximum entropy deep reinforcement learning with a stochastic actor,” in *International conference on machine learning*, pp. 1861–1870, PMLR, 2018.
- [27] S. Fujimoto, H. Hoof, and D. Meger, “Addressing function approximation error in actor-critic methods,” in *International conference on machine learning*, pp. 1587–1596, PMLR, 2018.
- [28] J. Schulman, F. Wolski, P. Dhariwal, A. Radford, and O. Klimov, “Proximal policy optimization algorithms,” *arXiv preprint arXiv:1707.06347*, 2017.
- [29] G. Brockman, V. Cheung, L. Pettersson, J. Schneider, J. Schulman, J. Tang, and W. Zaremba, “Openai gym,” *arXiv preprint arXiv:1606.01540*, 2016.
- [30] M. L. Puterman, *Markov decision processes: discrete stochastic dynamic programming*. John Wiley & Sons, 2014.